NOTICE

CERTAIN DATA CONTAINED IN THIS DOCUMENT MAY BE DIFFICULT TO READ IN MICROFICHE PRODUCTS.

UCRL-CR--106037

DE91 005199

SUPERCONDUCTING ENERGY GAP and NORMAL STATE CONDUCTIVITY of a SINGLE DOMAIN $Y_1Ba_2Cu_3O_7$ CRYSTAL.

Z. Schlesinger, R. T. Collins, F. Holtzberg, C. Feild and S. H. Blanton
IBM T. J. Watson Research Center
Yorktown Heights, New York 10598

U. Welp(1,2), G. W. Crabtree(2) and Y. Fang(2)
1.Science and Technology Center for Superconductivity
2.Materials Science Division, Argonne National Lab
Argonne, Illinois 60439

J. Z. Liu
Department of Physics,
University of California, Davis CA 95616

ABSTRACT

Using polarized reflectivity measurements of single domain crystals, we are able to distinguish chain and plane contributions to the infrared conductivity of $Y_1Ba_2Cu_3O_7$. A substantial chain contribution to $\sigma(\omega)$ persisting to low frequency and temperature is observed. For the intrinsic conductivity of the CuO_2 planes a superconducting energy gap of 500 cm^{-1} ($2\Delta/kT_c \simeq 8$) is evident in the infrared data, while the normal state conductivity drops much more slowly with ω than the ordinary Drude form, and can be described in terms of a scattering rate $\hbar/\tau^* \sim kT + \hbar\omega$ at low frequency. The former result ($2\Delta/kT_c \simeq 8$) suggests substantial suppression of T_c; the latter, that $Y_1Ba_2Cu_3O_7$ is not an ordinary Fermi liquid.

The essential feature common to all the cuprate superconductors(1) is the presence of CuO_2 planes. As they are doped away from half-filling, these planes evolve from highly correlated insulators, to quasi 2-dimensional conductors of unknown character with very high superconducting transition temperatures. The importance of studying the intrinsic dynamics of the carriers within the planes cannot be overstated. In this letter we report infrared measurements of single domain (untwinned) crystals of $Y_1Ba_2Cu_3O_7$. We are able to isolate, for the first time, the low frequency conductivity associated exclusively with the CuO_2 planes, and thus address fundamental questions regarding the intrinsic superconducting energy gap and normal state dynamics.

A superconducting energy gap of $2\Delta \simeq 8kT_c$ (500 cm^{-1}) was originally reported in 1987 (2), based on infrared measurements of high quality ($T_c \gtrsim 91$ K) twinned $Y_1Ba_2Cu_3O_7$ crystals. While subsequent work has supported this original identification(3-7), evidence for an energy gap of conventional magnitude ($2\Delta/kT_c \simeq 3.5$) has also been reported(8), as well as the claim that one cannot see a gap in $Y_1Ba_2Cu_3O_7$ with infrared measurements(9). In the present work on single domain crystals, we are able to distinguish chain and plane contributions to the conductivity. For the CuO_2 planes a superconducting energy gap of 500 cm^{-1}, which is isotropic within the a-b plane, is evident in the infrared data. The unusually large value of the gap relative to T_c, $2\Delta/kT_c \simeq 8$, suggests a substantial suppression of T_c in $Y_1Ba_2Cu_3O_7$, possibly due to strong inelastic pair-breaking scattering in the normal state.

We also measure, for the first time, the intrinsic normal state conductivity of the CuO_2 planes, which is peaked at $\omega = 0$ and drops unusually slowly as a function of frequency. This behavior can be described in terms of a scattering rate which is highly frequency dependent. $\hbar/\tau^* \simeq 0.6(\pi kT + \hbar\omega)$. Such a scattering rate may indicate that $Y_1Ba_2Cu_3O_7$ is "at the edge of the regime in which a Fermi liquid theory is well-defined", as we have previously suggested(4,10). This concept(11), and its relation to a number of experiments(10-12), have been discussed by Anderson (11) and by Varma et al.(13).

Regarding the distribution of holes between the planes and chains, we find that slightly more than half of the conductivity in the infrared is associated with the chains. This result suggests a high concentration of holes on the chains, and is consistent with roughly 0.25 holes per plane Cu and 0.5 holes per chain Cu(14).

The samples used in these experiments are single domain crystals of $Y_1Ba_2Cu_3O_7$ with $T_c \gtrsim 90$ K and transition widths of ~1 K, measured by d.c. magnetization at 1 Gauss. Lateral sample dimensions range from 1 to 2.5 mm (comparable to that of the twinned crystals that we have studied previously(5,6,10)), with thicknesses of ~100 μ. The single domain nature of the sample is obtained via a post-growth anneal under uniaxial stress(15). Normal incidence reflectivity is measured in the infrared and optical range with polarized radiation using an interferometer (for the infrared range) and a grating spectrometer (for the near-infrared and visible). For each frequency range, an appropriate polarizer is placed in the incident beam approximately 50 to 100 mm from the sample. The resulting reflectivity spectra, which extend up to 25,000 cm^{-1}, are Kramers-Kronig transformed to obtain the $\sigma_1(\omega)$ and $\varepsilon_1(\omega)$ for each polarization using termination procedures described previously(6).

In fig 1 conductivity spectra in the normal state (T = 100 K) are shown for the incident infrared electric field parallel to the $\hat{a}$ axis (solid curve) and the $\hat{b}$ axis (dashed curve). The corresponding reflectivities for $\vec{E}\|\hat{a}$ (solid) and $\vec{E}\|\hat{b}$ (dashed) are shown in the insert. From these reflectivities we obtain screened plasma frequencies of about 7,000 cm^{-1} and 12,000 cm^{-1}, respectively, in reasonable agreement with the results of Koch, Geserich and Wolf(16) and Petrov et al.(17). The dotted curve shown in fig 1 is the excess conductivity in the $\hat{b}$ direction, i.e., $\sigma_b(\omega)$-$\sigma_a(\omega)$.

In $Y_1Ba_2Cu_3O_7$, in addition to the CuO_2 planes, there are linear CuO chains which are oriented along the $\hat{b}$ axis. For the incident infrared electric field parallel to the $\hat{a}$ axis, one probes only the conductivity of the planes, however, for $\vec{E}\|\hat{b}$ one must consider possible contributions to $\sigma(\omega)$ from the chains as well. Neglecting interactions between the chains and planes, the $\hat{b}$ axis conductivity is the sum of distinct chain and plane contributions, thus we may identify the difference between the $\hat{b}$ and $\hat{a}$ axis conductivities, shown in fig 1, with the conductivity of the chains(18). Integrating $\sigma_1(\omega)$ as a function of frequency, (from 0 up to any cutoff between ~4,000 and 15,000 cm^{-1}), one finds that 50-60% of the infrared conductivity for $\vec{E}\|\hat{b}$ is associated with the chains, suggesting that roughly half of the holes are on the chains(19). A hypothetical extrapolation to $\omega=0$ as a constant would suggest a ~10 - 30 % anisotropy in ρ_{dc} due to the chain conductivity.

Turning our attention to the lower part of our frequency range, in fig 2 polarized reflectivity spectra in the normal and superconducting state are shown for two samples. One observes that for $\vec{E}\|\hat{a}$ the reflectivity in the superconducting state (R_s) is very high (~100 %) for $\omega \lesssim 500$ cm^{-1}, while for $\vec{E}\|\hat{b}$, R_s is much lower (and clearly less than 100 %) in the same frequency range. These differences are most readily understood by examining the conductivity spectra, discussed in the next paragraph. A comparison of the reflectivity spectra in parts a) and c), and in parts b) and d) indicates that the data are reproducible. As in the twinned crystals(2-6), the differences between the normal and superconducting state spectra evolve rapidly between about 90 K and 60 K for both polarizations, and the superconducting to normal state reflectivity ratios (R_s/R_n) are peaked at ~500 cm^{-1} for both the pure $\hat{a}$ and $\hat{b}$ polarizations, as well as for polarizations intermediate between $\hat{a}$ and $\hat{b}$. Below about 55 K there is no appreciable temperature dependence in the infrared data.

In figure 3 the conductivities corresponding to the polarized reflectivity spectra of fig 2 (a and b) are shown. The error bars shown in fig 3a represent the uncertainty in $\sigma_{1s}(\omega)$ associated with shifting the reflectivity up or down by 0.5 % (for a total excursion of 1 %). For $\vec{E}\|\hat{a}$ the superconducting state conductivity rises from 0±100 to 1200 (Ωcm)$^{-1}$ beginning at the threshold frequency of 500 cm^{-1}. This threshold is also observed for $\vec{E}\|\hat{b}$, however, for this polarization the entire spectrum is displaced vertically by roughly 1600 (Ωcm)$^{-1}$. We interpret this displacement as due to the additional conductivity of the chains for $\vec{E}\|\hat{b}$. These results thus indicate the presence of a 500 cm^{-1} energy gap in both the $\hat{a}$ and $\hat{b}$ directions (associated with the CuO_2 planes), and a chain conductivity (with no 500 cm^{-1} gap) which persists below 500 cm^{-1} for $\vec{E}\|\hat{b}$. From the area missing from $\sigma_{1s}(\omega)$ relative to $\sigma_{1n}(\omega)$ (for either polarization) one obtains an estimate for the penetration depth of $\lambda \simeq 1500$ Å, in good agreement with μsr, magnetization and previous estimates using infrared data(6). The observation of an isotropic gap for the CuO_2 planes is consistent with the isotropy of H_{c2} recently measured by Welp et al.(15).

The chain conductivity thus accounts for the absorption present below 500 cm^{-1} in the superconducting state for $\vec{E}\|\hat{b}$, and is also sufficient to account for a similar low frequency absorption observed in twinned crystals(5-9) (as we have previously suggested(5,6)). Our results show no evidence for a gap in the chain conductivity in the frequency range $\omega \gtrsim 150$ cm^{-1}. Results of Pham et al.(20) and

Miller et al.(21) indicate finite absorption down to even lower frequencies in twinned samples, suggesting an absence of evidence for a chain gap to below 50 cm^{-1}.

For the 500 cm^{-1} gap of the CuO_2 plane conductivity, both the magnitude of the gap relative to T_c ($2\Delta/kT_c \simeq 8$) and the temperature dependence are unusual. The temperature dependence of the energy gap will be discussed in more detail in a subsequent publication. Here we would like to mention that the energy scale of the gap appears to remain large as T_c is approached from below, while, the area missing from the conductivity (and hence the superfluid density) decreases gradually between about 55 K and T_c. These observations are consistent with earlier work on twinned crystals(6), and allow a reconciliation of the gradual growth of the penetration depth near T_c(22) with the large magnitude of 2Δ. The manner in which the conductivity "fills in" as T_c is approached from below may be interpretable in terms of an increase in $Im\{\Delta\}$, or may have an even more exotic origin. The unusual temperature dependence of the infrared gap may also be relevant to understanding the observed absence of a coherence peak in nuclear relaxation rates(23), since both a rapid growth of $Re\{\Delta\}$ and a large value of $Im\{\Delta\}$ tend to supress the coherence peak(24).

The normal state conductivity of the CuO_2 planes, shown in fig 4a, falls much less rapidly with frequency than would a Drude conductivity with a fixed scattering rate. One approach to the normal state has been to divide $\sigma(\omega)$ into two parts, one associated with a ordinary Drude term, the other with a mid-infrared mode or modes(9). Such a separation may be relevant at energies where interband or excitonic contributions to $\sigma(\omega)$ are significant (e.g., $\omega \gtrsim 5000$ cm^{-1}). At lower frequencies, however, no clear reason (or method) exists for separating $\sigma(\omega)$ into distinct parts. In this frequency range a formulation in terms of a

Drude conductivity with frequency dependent scattering rate(8,10), $1/\tau^*$, reveals a fundamental relationship between the d.c. and infrared scattering rates. (A similar approach has been used by Webb et al.(25) to study heavy fermions, where $1/\tau^* \propto \omega^2$ and $\rho \propto T^2$.) For the CuO_2 plane conductivity of $Y_1Ba_2Cu_3O_7$, this approach leads to a scattering rate, as shown in fig 4b, of $1/\tau^* \simeq 0.6\omega$, *which is linear in frequency*. This result appears to be fundamentally related to the linear temperature dependence of the d.c. resistivity. One can express this relationship in terms of a generalized expression for the T and ω dependence of the scattering rate,

$\hbar/\tau^* \simeq 0.6(\pi kT + \hbar\omega)$ (or, $\hbar/\tau^* \simeq 0.6\max\{\pi kT, \hbar\omega\}$).

One can view this broadly increasing scattering rate as arising from an interaction of the carriers with a broad excitation spectrum. We find that a good fit to the normal state conductivity (shown in fig 4a) is obtained by allowing the carriers to interact with a spectrum which is constant up to 1000 cm^{-1}, with an appropriate low ω termination. Since 1000 cm^{-1} is roughly J (the magnetic exchange energy), one may speculate that an interaction between the carriers and a spin-related excitation spectrum is responsible for the novel normal state dynamics of the CuO_2 planes. More generally, the linear frequency dependence of $1/\tau^*$(4,10), the related linear temperature dependence of the resistivity, and the broad Raman background signal(12) (as well as nulear relaxation and photoemission data), appear to provide experimental evidence for the unusual nature of the cuprates in the normal state(11,13,26).

In summary, we have measured both the chain and plane contributions to $\sigma(\omega)$ in $Y_1Ba_2Cu_3O_7$. Several features of the experimental data stand out:

1) the normal state conductivity of the CuO_2 planes falls unusually slowly with frequency, thus there is substantially more conductivity for $\omega \gtrsim 200$ cm^{-1} than one would expect for an ordinary Drude metal,

2) the superconducting state conductivity of the CuO_2 planes exhibits an absorption threshold at ~ 500 cm^{-1}, just below which $\sigma_{1s}(\omega) \simeq 0$,

3) as T_c is approached, the disappearance of this energy gap occurs in a highly unconventional manner, and

4) there is a substantial chain conductivity in the infrared, however, we find no evidence for a gap in this chain conductivity in the frequency range $\omega \gtrsim 150$ cm^{-1}.

Acknowledgements:

The authors acknowledge valuable conversations with P. W. Anderson, N. E. Bickers, D. J. Scalapino, P. M. Horn, E. Abrahams, P. B. Littlewood, A. J. Mills, and C. M. Varma. This work was supported by the U. S. Department of Energy, Basic Energy Science, under contract W-31-109-ENG-38 (GWC, YF, JZL), for Lawrence Livermore National Laboratory under contract W-7405-ENG-48 (JZL at U.C. Davis), and the National Science Foundation--Office of Science and Technology Centers, under contract STC-8809854 (UW).

References

1. J. G. Bednorz and K. A. Müller, Z. Phys. B **64** 189 (1986)
2. Z. Schlesinger, R. T. Collins, D. L. Kaiser, and F. Holtzberg, Phys. Rev. Lett. 59, 1958 (1987);
3. Z. Schlesinger, R. T. Collins, D. L. Kaiser, F. Holtzberg, G. V. Chandrashekhar, M. W. Shafer, and T. M. Plaskett, Physica C 153, 1734 (1988).
4. R. T. Collins, Z. Schlesinger, F. Holtzberg, P. Chaudari, and C. Feild, Oberlech workshop, Austria (1988).
5. R. T. Collins, Z. Schlesinger, F. Holtzberg and C. Feild, Phys. Rev. Lett. 63, 422 (1989).
6. Z. Schlesinger, R. T. Collins, F. Holtzberg, C. Field, G. Koren and A. Gupta, Phys. Rev. B, June 1, (1990).
7. J. Schutzmann, W. Ose, J. Keller, K. F. Renk, B. Roas, L. Schultz and G. Saemann-Ischenko, Europhysics Lett. 8, 679 (1989)
8. G. A. Thomas, J. Orenstein, D. H. Rapkine, M. Capizzi, A. J. Millis, R. N. Bhatt, L. F. Schneemeyer and J. V. Waszczak, Phys. Rev. Lett. **61**, 1313 (1988).
9. K. Kamaras, S. L. Herr, C. D. Porter, N Tache, D. B. Tanner, S. Etemad, T. Venkatesan, E. Chase, A. Inam, X. D. Wu, M. S. Hegde, and B. Dutta, Phys. Rev. Lett. **64**, 84 (1990); erratum, ibid, page 1962
10. R. T. Collins, Z. Schlesinger, F. Holtzberg, P. Chaudari and C. Feild, Phys. Rev. B. 39, 6571 (1989)
11. P. W. Anderson, in Strong Correlation and Superconductivity, edited by H. Fukuyama, S. Maekawa and A. Malozamoff (Springer-Verlag, Berlin, 1989)
12. M. V. Klein, ibid
13. C. M. Varma, P. B. Littlewood, S. Schmitt-Rink, E. Abrahams and A. E. Ruckenstein, Phys. Rev. Lett. 63, 1996 (1989); ibid, vol. 64, 497 (1990) (erratum)
14. Y. Tokura, J. B. Torrance, T. C. Huang and A. I. Nazzal, Phys. Rev.B. 38, 7156 (1988).
15. U. Welp, G. Grimsditch, H. You. W. K. Kwok, M. M. Fang, G. W. Crabtree, and J. Z. Liu, Physica C 161, 1 (1989)
16. B. Koch, H. P. Geserich and TH. Wolf, Solid State Commun. 71, 495 (1989)

17. M. P. Petrov, A. I. Grachev, M. V. Krasin'kova, A. A. Nechitailov, V. V. Poborchii, S. I. Shagin and S. V. Miridonov, JETP Lett. 50, 29 (1989)

18. This relies on the assumption that the plane contribution to $\sigma(\omega)$ is isotropic, which is reasonable since the plane Cu-O bond lengths in the $\hat{a}$ and $\hat{b}$ directions are virtually identical (the 2% lattice constant difference is associated with buckeling).

19. If one assumes that the chain and plane band masses are roughly equal (as would be the case if both are dominated by the oxygen bandwidth), then this result implies ~0.5-0.6 holes per chain Cu, and 0.25-0.2 holes per plane Cu (total of 1 hole per unit cell).

20. T. Pham, H. D. Drew, S. H. Moseley and J. Z. Liu, Phys. Rev. B, to be published

21. D. Miller and P. L. Richards, private communication

22. S. Sridhar, Dong-Ho Wu and W. Kennedy, Phys. Rev. Lett. 63, 1873 (1989)

23. P. C. Hammel, M. Takigawa, R. H. Heffner, Z. Fisk and K. C. Ott, Phys. Rev. Lett. 63, 1992 (1989)

24. L. Coffey, Phys. Rev. Lett. 64, 1071 (1990); personal communication N. E. Bickers and D. J. Scalapino; K. Kuroda and C. M. Varma, preprint

25. B. C. Webb, A. J. Sievers and T. Mahalisin, Phys. Rev. Lett.57, 1951 (1986)

26. J. C. Phillips, Phys. Rev. B 40, 7346 (1989)

FIGURE CAPTIONS

Figure 1: The (real part of the) conductivity in the normal state (T = 100 K) is shown for the incident infrared electric field parallel to the $\hat{a}$ axis (solid) and $\hat{b}$ axis (dashed). The corresponding $\hat{a}$ and $\hat{b}$ axis reflectivities are shown in the insert. The difference spectrum, $\sigma_b(\omega)$-$\sigma_a(\omega)$, (associated with the chain conductivity) is shown by the dotted curve.

Figure 2: Polarized reflectivity spectra in the normal (T = 100 K, dashed curves) and superconducting state (T = 35 K, solid curves) are shown for two untwinned $YBa_2Cu_3O_7$ crystals. Parts (a) and (b) are from sample 1; parts (c) and (d) are from sample 2. These data show good reproducibility, and a dramatic difference between the superconducting state reflectivity for $\vec{E}\|\hat{a}$ and $\vec{E}\|\hat{b}$. (The sharp minima in R_s at ~550 cm^{-1} ($\vec{E}\|\hat{b}$) and 590 cm^{-1} ($\vec{E}\|\hat{a}$) are direct optic phonon absorptions.)

Figure 3: a) The conductivity of the CuO_2 planes (measured with $\vec{E}\|\hat{a}$) is shown in the normal (T = 100 K) and superconducting (35 K) states, along with a fit (dotted curve) to the normal state spectrum. (These data correspond to the reflectivity data shown in fig 2a.) The superconducting state conductivity, $\sigma_{1s}(\omega)$, is ~0 up to an excitation threshold of 500 cm^{-1}. The error bars indicate the uncertainty in $\sigma_{1s}(\omega)$ associated with shifting R_s by $\pm$0.5 %.
b) The conductivity measured for $\vec{E}\|\hat{b}$, which includes contributions from both the chains and planes, is shown for T = 100 K (dashed) and 35 K (solid). For this polarization, $\sigma_{1s}(\omega)$ exhibits a similar threshold at ~500 cm^{-1}, with the entire spectrum is shifted upward by about 1600 $(\Omega cm)^{-1}$ due to the conductivity of the chains.

Figure 4: The scattering rate, $1/\tau^*$ (solid curve), and the effective mass, m^* (dashed curve), extracted from the measured $\hat{a}$ axis conductivity at $T = 100$ K (shown in fig 3a)) are shown. The broadly increasing scattering rate reflects the fact that the conductivity drops unusually slowly with increasing ω in the normal state. Both the linearity of the scattering rate vs. ω and the large magnitude of the inelastic rate ($1/\tau^* \sim \omega$) are highly unconventional.

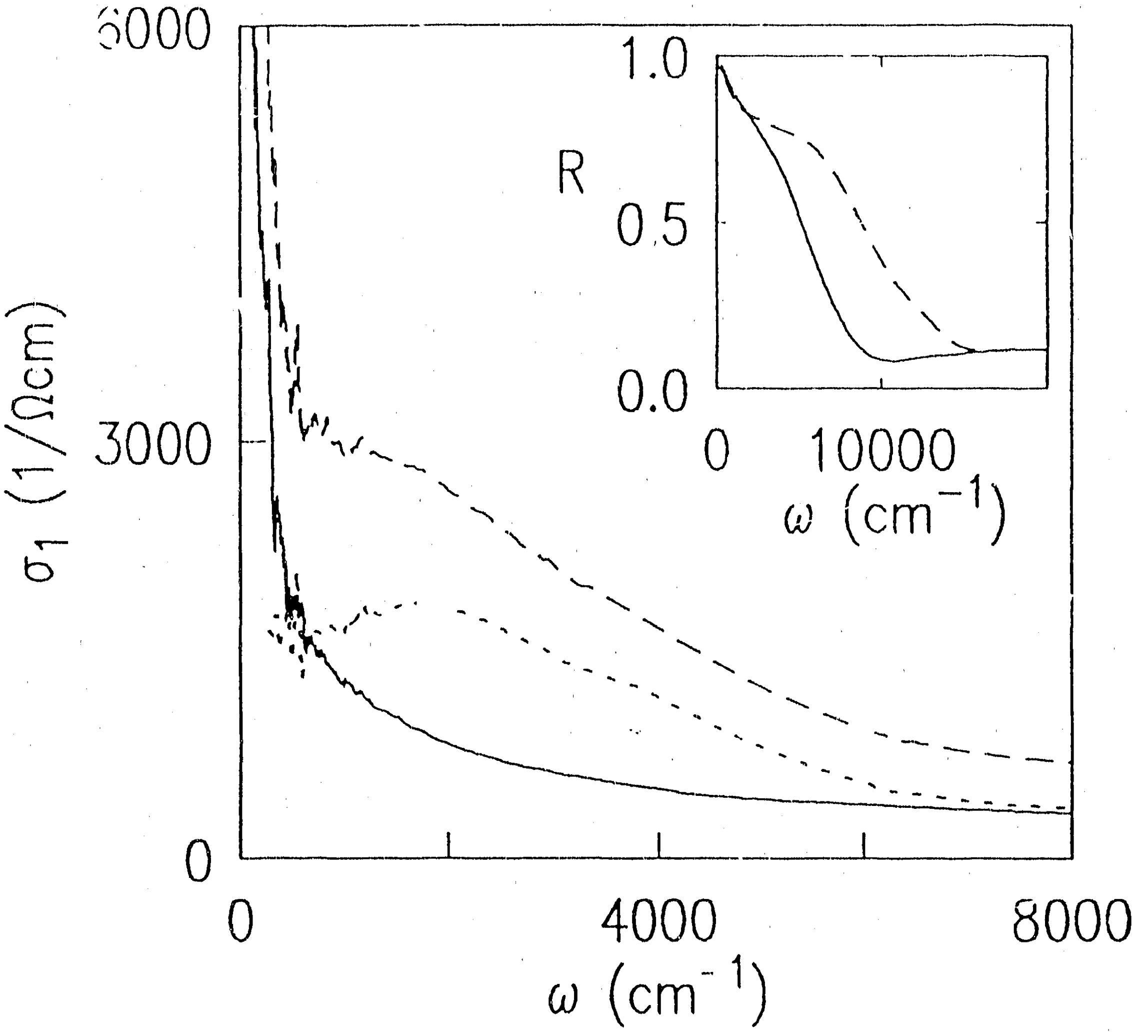

Fig 1

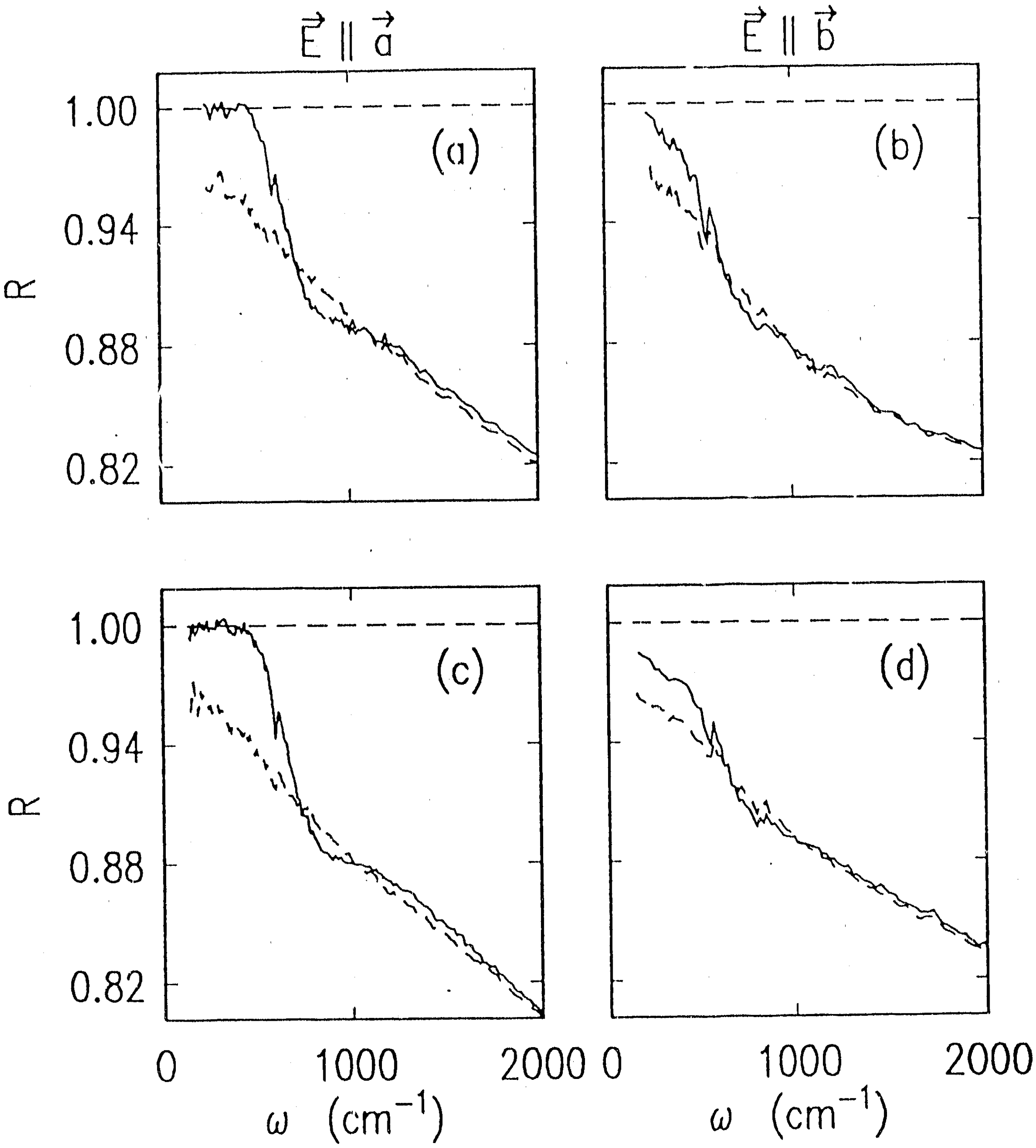
$\vec{E} \parallel \vec{a}$
$\vec{E} \parallel \vec{b}$
(a)
(b)
(c)
(d)
R
1.00
0.94
0.88
0.82
0
1000
2000
ω (cm^{-1})

Figure 7

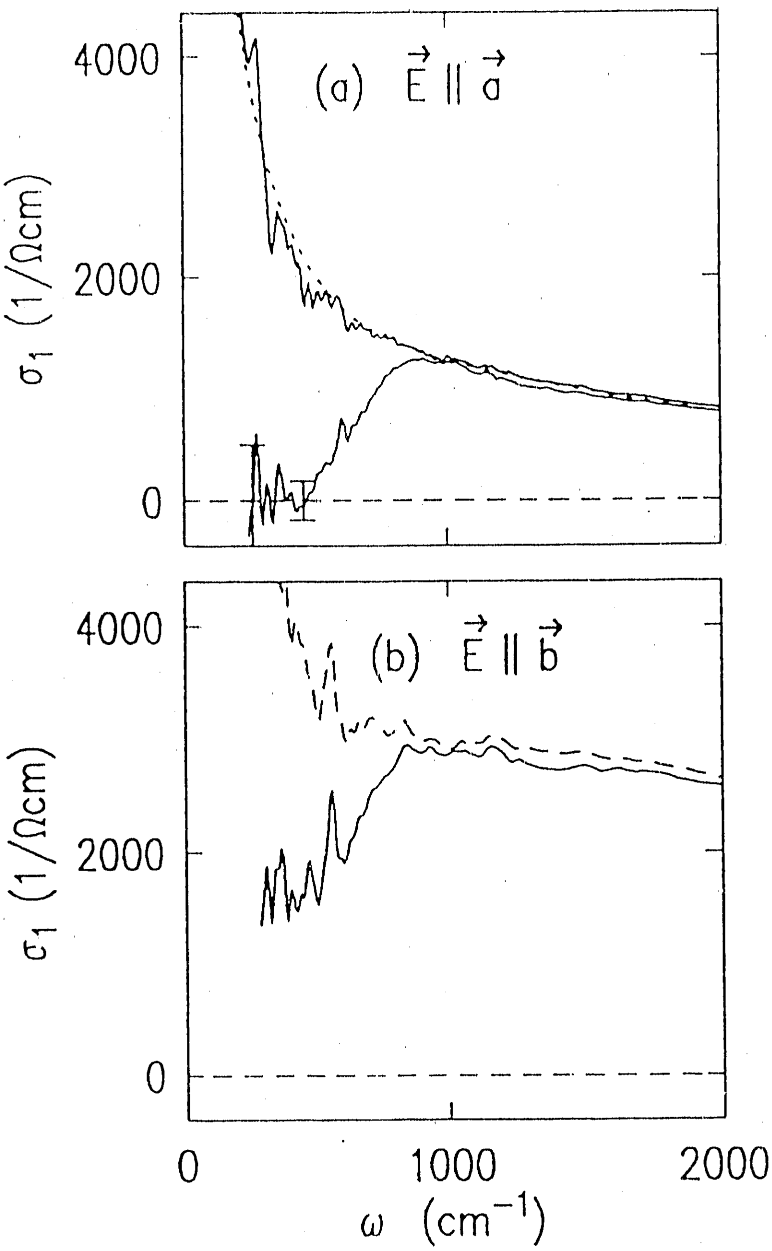
4000
2000
0
(a) $\vec{E} \parallel \vec{a}$
σ_1 (1/Ωcm)
4000
2000
0
(b) $\vec{E} \parallel \vec{b}$
σ_1 (1/Ωcm)
0
1000
2000
ω (cm^{-1})

figure 3

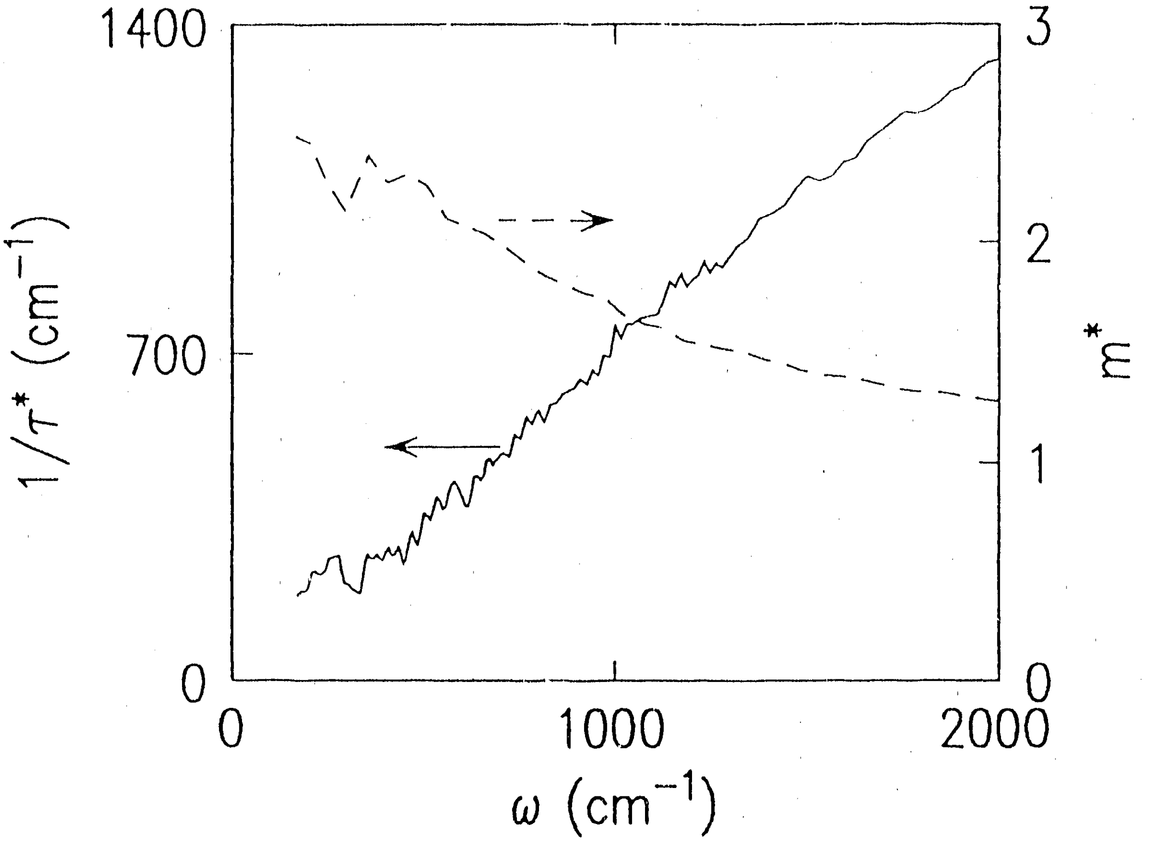

figure 4

END

DATE FILMED

01/10/91